Electronic Supplementary Material (ESI) for RSC Advances.
This journal is © The Royal Society of Chemistry 2015

Supporting Informations

Enhanced Catalytic and Antibacterial Activities of Silver Nanoparticles Immobilized on Poly(*N*-vinyl pyrrolidone)-Grafted Graphene Oxide

Shikha Singh,[a] Ravi Kumar Gundampati,[b] Kheyanath Mitra,[a] K. Ramesh,[a,c] Medicherla V. Jaganaddam,[b] Nira Misra,[c] Biswajit Ray*[a]

[a]*Department of Chemistry, Faculty of Science, Banaras Hindu University, Varanasi – 221005, India*
[b]*Molecular Biology Unit, Institute of Medical Science, Banaras Hindu University, Varanasi – 221005, India*
[c]*School of Biomedical Engineering, Indian Institute of Technology (Banaras Hindu University), Varanasi-221005, India*

Corresponding author. Email: biswajitray2003@yahoo.co.in

S1 Raman spectra of GO, GO-N_3 and GO-PNVP

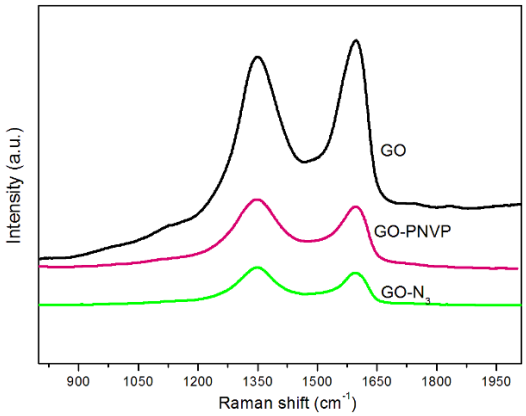

Fig. S-1 Raman spectra of GO, GO-N_3 and GO-PNVP.

GO-PNVP shows the shift of D and G band from 1348.1 and 1597.3 cm^{-1} to 1347 and 1595 cm^{-1}. Furthermore, the ratio of (I_D/I_G) increase gradually from GO (0.947), GO-N_3 (1.044) GO-PNVP (1.055) revealing the increased degree of functionalisation.[1]

S2 Fitted and deconvoluted XPS spectra of Br(3d), N(1s) and S(2p)

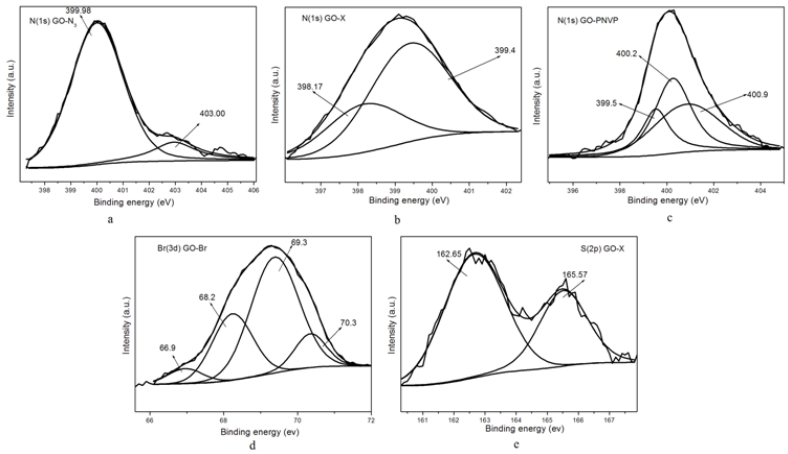

Fig. S-2 Fitted and deconvoluted XPS spectra of (a) N(1s) GO-N_3 (b) N(1s) GO-X (c) N(1s) GO-PNVP (d) Br(3d) GO-Br and (e) S(2p) GO-X.

N (1s) XPS spectra of GO-N_3 exhibited the peak at 403.00 eV attributed to the electron deficient inner nitrogen of the azide and the peak at 399.9 eV to electron rich outer nitrogen agreement with previous result for azide peak locations.[2] N (1s) XPS spectra of GO-X exhibited two peaks at 398.17 and 399.4 eV corresponding to N^*-N=N in 1,2,3 triazole ring and N^*=N in 1,2,3 triazole ring and thus confirmed the functionalization via the click reaction**.** N(1s) XPS spectra of GO-PNVP exhibited three peaks at 399.5, 400.2 and 400.9 eV corresponding to N^*-N=N in the 1,2,3 triazole ring, N^*=N in the 1,2,3 triazole ring and O=C-N^* from the pyrolidone ring[3] respectively. The Br (3d) XPS spectra of GO-Br exhibited four peak originates from two different doublets superimposed in such a way that peak at lower binding energy corresponding to the ionic state of Br (negatively charged bromine species) which are most probably absorbed Bromine anions of bromine salts with triethylamine while, the upper one is associated with covalently bonded Br.[4] The S (2p) XPS spectra of GO-PNVP exhibited two peak first at 162.65 eV is assigned to the (-S) of the ethyl xanthate groups[5] second, peak at 165.4 eV revealed that the part of sulphur (-S) in ethyl xanthate groups have been oxidised to S(VI).

S3 XRD spectra of GO and PNVP grafted GO

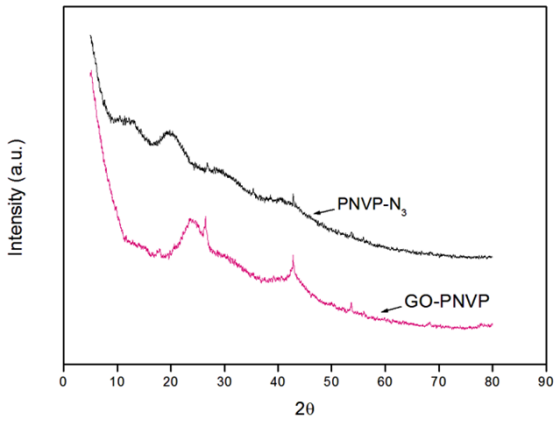

Fig. S-3 XRD spectra of GO and GO-PNVP.

Characteristic diffraction peak of PNVP appeared in GO-PNVP confirmed the successful grating of PNVP onto the GO.

S4 Thermal study of GO, GO-PNVP and PNVP

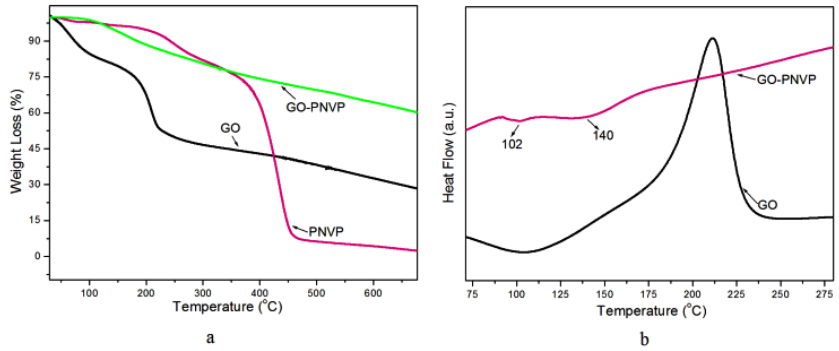

Fig. S-4 (a) TGA and (b) DSC Thermogram of GO, GO-PNVP and PNVP

Graphene oxide shows significant weight loss at 200 °C due to the presence of most labile oxygenated groups (hydroxyl, epoxy in the plane). PNVP exhibit good thermal stability until 400 °C. However, GO grafted with PNVP (GO-PNVP) delayed in the weight loss of GO it may be due to the thermal shielding effect caused by the existence of PNVP.[6] DSC curves of GO shows a degradation peak at 182.65 °C. This phenomenon principally ascribed more oxidation and longer exfoliation, thus decomposition temperature.[7] GO-PNVP show a sharp transition at 102 °C is due to the relaxation of its pyrolidone group. The secondary transition temperature at 143 °C is due to the glass transition temperature (T_g) of the backbone chain of PNVP.[8] All these reveal successful grafting of PNVP.

S5 UV-Vis spectra of (a) GO and GO-Ag 40 (b) GO-PNVP and GO-PNVP Ag 40

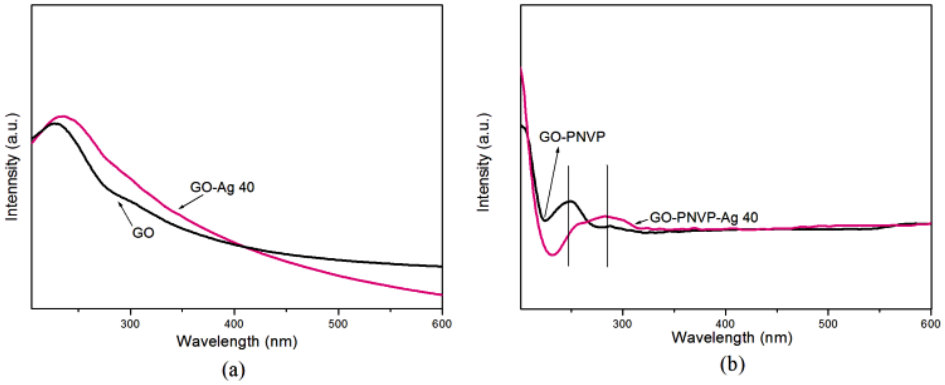

Fig. S-5 UV-Vis spectra of (a) GO and GO-Ag 40 (b) GO-PNVP and GO-PNVP Ag 40

The characteristics peak of 231 nm of the reference sample (GO-Ag 40) was broadened compared to those of the GO sample. This broadening suggest the charge transfer interactions between GO and the Ag nanoparticals reveals successful formation of Silver nanoparticals on to the graphene oxide. Whereas, GO-PNVP exhibited two peaks first at 248 nm second at 290 nm arise from n-π* transition of C=O band of pyrolidone rings both peaks were shifted to higher wavelength in case of GO-PNVP Ag 40 suggesting successful incorporation of nanoparticles into the substrate.

Table S-6 Average size of Nanoparticles Calculated using SEM

Sample	SEM Average Size (nm)
GO-Ag 40	58
GO-Ag 95	102
GO-PNVP Ag 40	30
GO-PNVP Ag 95	15

S7 TGA Study of GO-Ag and GO-PNVP-Ag system

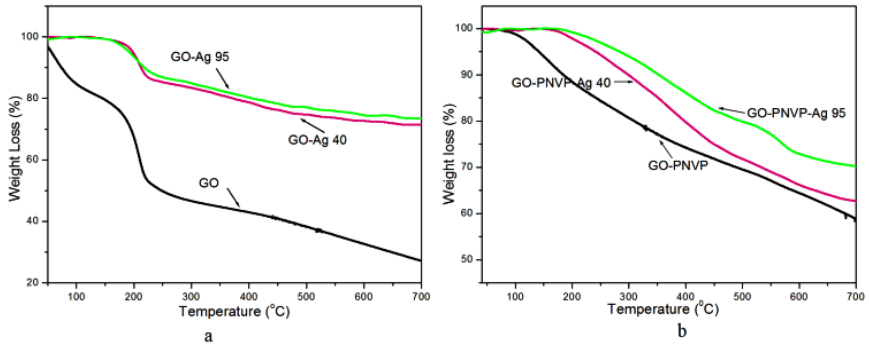

Fig. S-7 TGA Thermogram of (a) GO, GO-Ag 40 and GO-Ag 95 (b) GO-PNVP, GO-PNVP-Ag 40 and GO-PNVP-Ag 95.

TGA curve reflect the enhancement in thermal stability by Ag nanoparticles supported on GO and GO-PNVP.

S8 UV-Vis spectra Of the catalytic reduction of 4 NP to 4 AP over different catalyst

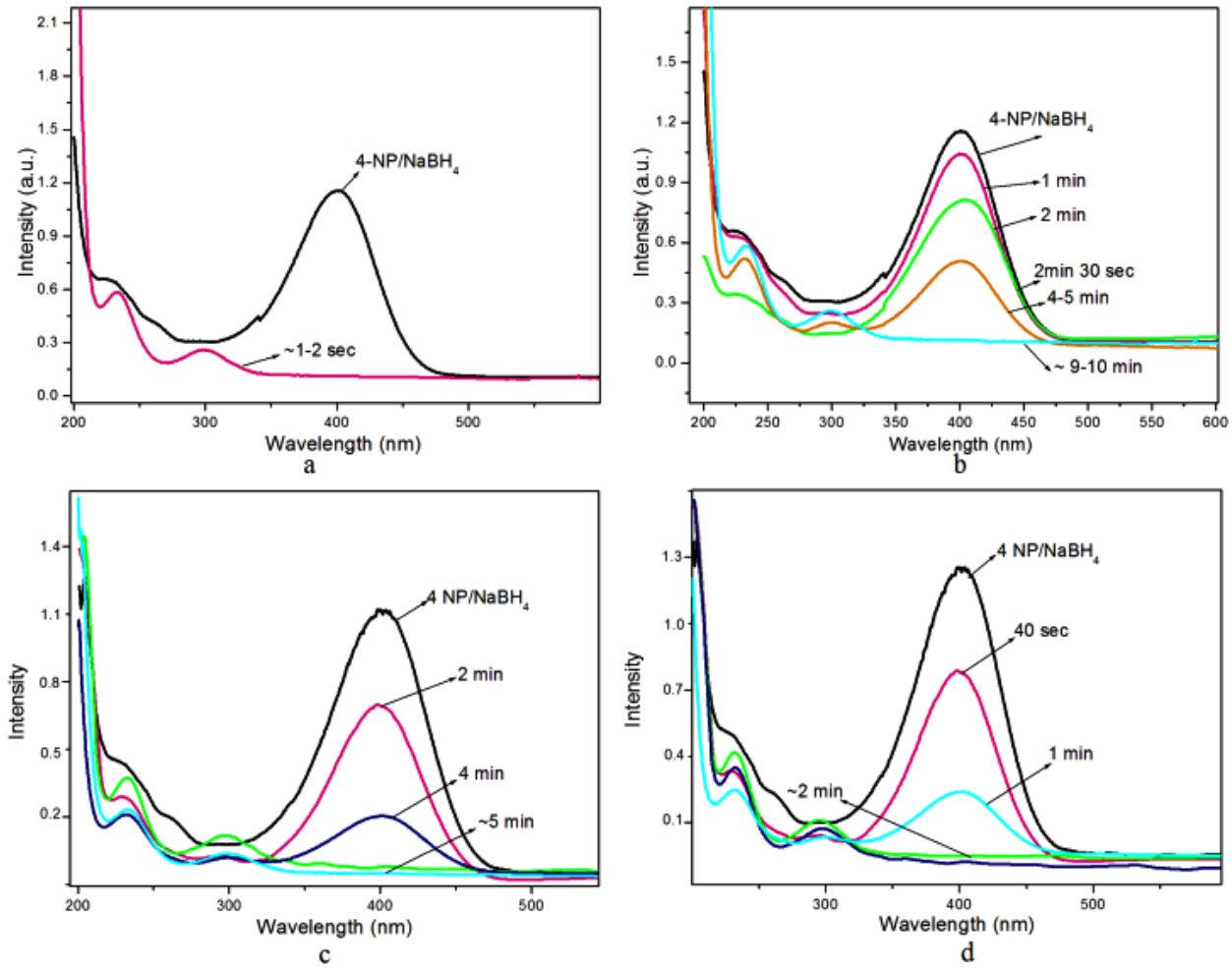

Fig. S-8 UV-Vis spectra of the catalytic reduction of 4 N to 4 AP over (a) GO-Ag 40 (b) GO-Ag 95 (c) GO-PNVP-Ag 40 and (d) GO-PNVP-Ag 95.

Table S-9 Literature Comparison of the Rate Constant for the reduction of p-nitropheno to p-aminophenol using Ag Nanoparticles immobilized on to Graphene oxide and its derivatives.

Sample Type	Rate constant (*k*) (s^{-1})	Ref
Ag-PRGO	3.74×10^{-3}	9
Ag-GO-Dopa	6.0×10^{-3}	10
RGO/Ag/CeO_2-4	3.3×10^{-3}	11
GO-Chit-Ag	5.5×10^{-3}	12
GO-Ag 40	**1.17**	*
GO-Ag 95	**3.6×10^{-3}**	*
GO-PNVP-Ag 40	**7.1×10^{-3}**	*
GO-PNVP-Ag 95	**1.9×10^{-2}**	*

Abbreviation for Table: Silver nanoparticles supported over partially reduced Grapheneoxide (Ag-PRGO), Siver supported over Dopamine functionalised Graphene oxide (Ag-GO-Dopa), Silver supported on Reduced Graphene oxide with CeO_2 Nanopartiles (RGO/Ag/CeO_2-4), Siver supported on Chitosan functionalized Graphene oxide (GO-Chit-Ag), * This work.

Table S-10 Antibacterial activities demonstrated by Graphene oxide and its derivatives against E. Coli and S. Aureus bacteria.

Sample Type	Sample Concentration (µg/mL)	Strains	Viable colonies of Bacteria before treatment (CFU/mL)	Duration (h)	Killing Rate (%)	Ref
PEI-rGO	958	E. coli	10^6	6	14.8	13
PNVP-Ag-NP	100	E. coli	10^6	6	86.4	13
PEI-rGO-AgNP	100	E. coli	10^6	6	93.7	13
PEI-rGO	958	S. aureus	10^6	6	20.5	13
PNVP-Ag-NP	100	S. aureus	10^6	6	89.2	13
PEI-rGO-AgNP	100	S.aureus	10^6	6	96.1	13
GO	45	E. coli	10^6 - 10^7	4	51.9	14
AgNP-GO	53.3	S. aureus	10^6 - 10^7	4	100	14

GO	45	E. coli	10^6 - 10^7	4	61.3	14
AgNP-GO	53.3	S. aureus	10^6 - 10^7	4	87.6	14
Gt	40	E. coli	10^6 -10^7	2	26.1	15
GtO	40	E. coli	10^6 -10^7	2	15.0	15
GO	40	E. coli	10^6 -10^7	4	89.7	15
rGO	40	E. coli	10^6 -10^7	4	74.9	15
GO-Ag	10	E. coli	10^4	2.5	94	16
GO-Ag	10	S. aureus	10^4	2.5	74	16
GO-PNVP	**5**	**E. coli**	**10^6**	**6**	**88.5**	*
GO-Ag 40	**5**	**E. coli**	**10^6**	**6**	**34.7**	*
GO-PNVP Ag 95	**5**	**E. coli**	**10^6**	**6**	**~100**	*
GO-PNVP	**5**	**S. aureus**	**10^6**	**6**	**85.2**	*
GO-Ag 40	**5**	**S. aureus**	**10^6**	**6**	**30.8**	*
GO-PNVP Ag 95	**5**	**S. aureus**	**10^6**	**6**	**~100**	*

* This work. All measurements were carried out in quadruplicate.

Abbreviation for Table: Polyethylene grafted Graphene oxide (PEI-rGO), Poly(*N*-vinyl pyrrolidone) stabilized silver Naoparticles (PNVP-Ag-NP), silver nanoparticles supported Graphene oxide (PEI-rGO-AgNP), Graphene oxide (GO), Silver nanoparticles Graphene oxide composites (AgNP-GO), Silver nanoparticles anchored Graphene oxide (GO-Ag), Graphite (Gt), Graphite oxide (GtO), Graphene oxide (GO), Reduced Graphene oxide (rGO)

Table S11. Values of Zeta Potential

Sample Name	Zeta Potential (mV)
GO	-50.70
GO-PNVP	-60.20
GO-Ag 40	-50.00
GO-Ag 95	-60.00
GO-PNVP-Ag 40	-35.70
GO-PNVP-Ag 95	-64.30

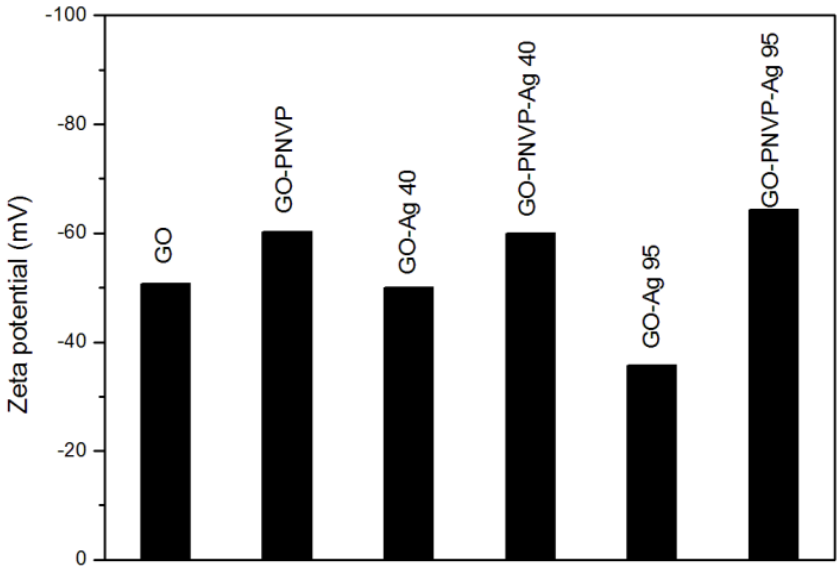

Figure S12. Zeta potentials of GO, GO-PNVP, GO-Ag 40, GO-PNVP-Ag 40, GO-Ag 95, and GO-PNVP-Ag 95 in deionized water

Reference:

1 M-C. Hsiao, S-H. Liao, M-Y. Yen, P-I. Liu, N-W. Pu, C-A. Wang and C-C. M. Ma, *ACS Appl. Mater. Interfaces*., 2010, **2** , 3092–3099.

2 S. Prakash, T. M. Long, J. C. Selby, J. S. Moore and M. A. Shannon, *Anal. Chem*., 2007, **7***,* 1661–1667.

3 C. Haensch, S. Hoeppener , U. S. Schubert, *Nanotechnology.*, 2008, **19**, 035703-035709.

4 L-P. Wang, Y-P. Wang, K. Yuan and Z-Q. Lei, *Polym. Adv. Technol.,* 2008, **19**, 285–290.

5 J. Li, L. Vaisman, G. Marom and J-K. Kim, *Carbon.,* 2007, **45**, 744-750.

6 Y. Yang, L. Ren, C. Zhang, S. Huang and T**.** Liu, *ACS Appl Mater Interfaces.,* 2011, **3**, 2779-2785.

7 L. Zhang, J. Liang, Y. Huang, Y. Ma, Y. Wang and Y. Chen, *Carbon*., 2009, **47**, 3365–3368.

8 V. K. Patel, N. K. Vishwakarma, A. K. Mishra, C. S. Biswas, P. Maiti and B. Ray, *Journal of applied polymer science.,* 2013, **127**, 4305–4317.

9 M-Q. Yang, X. Pan, N. Zhang and Y-J. Xu, *CrystEngComm.,* 2013, **15**, 6819–6828.

10 E. K. Jeon, E. Seo, E. Lee, W. Lee, M-K. Um and B.-S Kim, *Chem. Commun.,* 2013, **49**, 3392—3394.

11 Z. Jia, X. Shena, J. Yanga, G. Zhua and K. Chen. *Applied Catalysis B: Environmental.,* 2014*,* **144***,* 454– 46.

12 R. Rajesh, E. Sujanthi, S. S Kumar, and R. Venkatesan, *Phys. Chem. Chem. Phys.,* 2015, **17**, 11329—11340.

13 X. Cai, M. Lin, S. Tan, W. Mai, Y. Zhang, Z. Liang, Z. Lin and X. Zhang, *Carbon.,* 2012, **50**, 3407-3415.

14 Q. Bao, D. Zhang and P. Qi, *Journal of Colloid and Interface Science.,* 2011, **360**, 463–470.

15 S. Liu, T. H. Zeng; M. Hofman, E. Burcombe, J. Wei, R. Jiang, Jing. Kong and Y. Chen, *ACS Nano*., 2011, **5**, 6971–6980.

16 J. Tang, Q. Chen, L. Xu, S. Zhang, L. Feng, L. Cheng, H. Xu, Z. Liu and R. Peng, *ACS Appl. Mater. Interfaces,* 2013, **5**, 3867−3874.